

Testing solar neutrino MSW oscillations at low δm^2 through time variations of event rates in GNO and BOREXINO

G.L. Fogli ^a, E. Lisi ^a, D. Montanino ^b, and A. Palazzo ^a

^a *Dipartimento di Fisica and Sezione INFN di Bari,
Via Amendola 173, I-70126 Bari, Italy*

^b *Dipartimento di Scienza dei Materiali dell'Università di Lecce,
Via Arnesano, Collegio Fiorini, I-73100 Lecce, Italy*

Abstract

The Mikheyev-Smirnov-Wolfenstein (MSW) explanation of the solar neutrino problem is currently compatible with three distinct regions of the two-neutrino oscillation parameter space ($\delta m^2, \sin^2 2\theta$). We focus on the region with the lowest value of δm^2 ($\sim 10^{-7}$ eV²), which implies significant Earth regeneration effects for low-energy solar neutrinos. We point out that such effects are not only observable as *day-night* variations of neutrino event rates in the real-time BOREXINO experiment, but also as *seasonal* variations in the radiochemical Gallium Neutrino Observatory (GNO) at Gran Sasso. We present detailed calculations of the difference between winter and summer rates in GNO (six months averages) in excess of the trivial seasonal variation due to the Earth orbital eccentricity. We show that, within the low- δm^2 MSW solution, the net winter-summer GNO rate difference amounts to 4–6 SNU, with a dominant contribution from *pp* neutrinos. We also give analytical expressions for the winter and summer solar exposure functions at the Gran Sasso site.

PACS number(s): 26.65.+t, 13.15.+g, 14.60.Pq, 91.35.-x

I. INTRODUCTION

The available solar neutrino data from the Homestake (Cl) [1], GALLEX (Ga) [2], SAGE (Ga) [3], Kamiokande (K) [4], and Super-Kamiokande (SK) [5,6] experiments indicate consistently a significant ν_e flux deficit [7] with respect to the predictions of the Standard Solar Model (SSM) [8]. The Mikheyev-Smirnov-Wolfenstein (MSW) mechanism of neutrino oscillations in matter [9] represents a possible explanation of this deficit.

Recent global analyses of the data within the MSW mechanism for active 2ν oscillations [6,10,11] currently select three separate regions in the parameter space ($\delta m^2, \sin^2 2\theta / \cos 2\theta$), as shown in Fig. 1.¹ The three allowed regions are usually indicated [12] as “small mixing angle” (SMA), “large mixing angle” (LMA), and “low δm^2 ” (LOW) solutions.

The precise shape of the allowed regions in Fig. 1 is subject to changes due to fluctuations in the data, improvements in the SSM fluxes, and details of the statistical analysis. In particular, the LOW solution, which tends to overestimate the Cl rate and to underestimate the Ga rate, is a “borderline” case: it may be allowed (see, e.g., [6,10–15]) or excluded (see, e.g., [16–19]) at 99% C.L., as a consequence of relatively small variations in the data or in the theoretical predictions and their uncertainties. Notice that the recent *spectral* data from SK [5,6] do not show clear deviations from standard expectations, and are compatible with the LOW solution, which predicts small or null distortions of the SK time-energy distributions of events (see, e.g., Figs. 5–7 of Ref. [20] for $\delta m^2 \sim 10^{-7}$).

Clearly, the status of the LOW solution (as well as of the SMA and LMA solutions) can be firmly assessed only through more precise or new experimental data. Since the MSW physics scales as $\delta m^2 / E_\nu$, the low- δm^2 region is more properly tested through observations of the low-energy part of the solar neutrino spectrum. In particular, within the LOW solution the Earth regeneration effects [21] are rather large for Be and pp solar ν_e ’s (see, e.g., [15] and Fig. 9 of [19]). Such effects can be revealed as time variations of event rates in two, new-generation solar neutrino experiments at Gran Sasso: BOREXINO [22] (based on ν - e scattering) and the Gallium Neutrino Observatory (GNO) [23] (based on ν_e -Ga absorption). However, while the real-time experiment BOREXINO can observe *day-night* rate variations, the radiochemical GNO experiment can detect only long-term, *seasonal* variations related to the longer neutrino pathlength in the Earth during winter.²

In this work, we first revisit (Sec. II) the calculation of the night-day asymmetry expected in BOREXINO. Then we present (Sec. III) a detailed calculation of the winter-summer rate difference $R_W - R_S$ (six months averages) in GNO, with eccentricity effects removed. We show that, within the LOW solution, one expects $R_W - R_S \simeq 4\text{--}6$ SNU, with a dominant contribution from pp neutrinos. We conclude our work in Sec. IV, and give in the Appendix analytical formulae useful for winter and summer averages at the Gran Sasso site.

¹The results in Fig. 1 are derived by our analysis of solar ν data, updated as of summer ’99 conferences. The details are not relevant for the present work and are discussed elsewhere [11].

² See [24–26] for recent discussions and earlier references about MSW-induced seasonal effects. Extensive references to day-night effects can be found in [20].

II. DAY-NIGHT VARIATIONS IN BOREXINO

Figure 2 shows our calculation of the event rates (normalized to SSM unoscillated values) in BOREXINO during daytime (D) and nighttime (N), averaged over the year. The scales are the same as in Fig. 1. In particular, we adopt $\sin^2 2\theta / \cos 2\theta$ as abscissa, rather than the usual variable $\sin^2 2\theta$, in order to expand the plot in the region at large mixing, interesting for the LOW solution. The calculation includes updated neutrino fluxes, spectra, and production regions in the Sun [8], radiatively corrected differential cross sections [27] for ν_e and for the oscillating partners $\nu_{\mu,\tau}$, and BOREXINO detector technical specifications as in [28]. The ν_e survival probability is calculated taking into account an accurate Earth density profile [29], and is then averaged over nighttime as described in [20]. Each panel of Fig. 2 is sampled through a 100×100 grid.

The comparison of the yearly-averaged nighttime and daytime rates in Fig. 2 shows that day-night variations larger than 1% are expected in BOREXINO over three decades in δm^2 ($\sim 10^{-8}$ – 10^{-5} eV²), as a consequence of (mainly Be) neutrino regeneration in the Earth. The maximum night-day asymmetry can be as large as $\sim 40\%$ at $(\delta m^2/\text{eV}^2, \sin^2 2\theta) \simeq (3 \times 10^{-7}, 0.2)$ (similar results have been obtained in [12,30]). However, within the LOW solution of Fig. 1, the values expected for the asymmetry are smaller ($N - D/N + D \simeq 10$ – 20%). Although a 10% asymmetry seems to be sufficiently large for a clear detection in BOREXINO [30], this fact indicates that the Be neutrino energy is somewhat too high to test the LOW region with full-strength Earth regeneration effects. Therefore, the logical next step is to investigate the Earth regeneration effect in experiments sensitive to the lowest-energy (pp) neutrinos, namely, gallium absorption experiments.

III. SEASONAL VARIATIONS IN GNO

When the first solar neutrino results from GALLEX and SAGE became available, the authors of [15] pointed out that large *day-night* variations should be expected in such experiments within the LOW solution (which they called “region C”). However, such daily variations of the Ga event rate [31] are practically unobservable, being averaged out in each experimental run.³ Similarly, day-night effects for B and Be neutrinos are effectively smeared out in the Homestake (Cl) experiment [1], since early proposals of separate day-night extractions [35] have never been realized. Nevertheless, it was noted in several 1986-87 papers that “... a day-night difference, if it is sufficiently large, should reveal itself also in a summer-winter difference” [36] (see also [21,37]). However, given the limited statistics of the first-generation Ga and Cl experiment, the possibility of observing MSW-induced seasonal variations in radiochemical experiments was not (to our knowledge) further investigated.

³Future real-time observations of day-night effects for pp neutrinos might be possible through a recently proposed technique [32] based on ν_e absorption on Yb and Gd targets, as in the Low Energy Neutrino Spectroscopy (LENS) project [33]. Other projects (HERON, HELLAZ) focus on ν - e scattering in Helium [34]. Such proposals are not investigated in this work.

Here we fill this gap by showing that such possibility might become realistic in the second-generation, high-statistics GNO experiment at Gran Sasso, which should significantly improve the already excellent performance of its parent experiment GALLEX. In fact, we estimate that MSW-induced *seasonal* variations in the range $\sim 4 - 6$ SNU are expected in a Ga experiment (within the LOW solution). Such variations, which are below the GALLEX and SAGE detection sensitivities [16], might well be observed at GNO, where the prospective statistical error after one solar cycle amounts to $\lesssim 2$ SNU [23]. Indeed, the observation of the purely geometrical ($1/L^2$) seasonal variations due to the Earth orbit eccentricity represents one of the possible goals in GNO [23].

Being interested only in the nontrivial seasonal variations, we remove eccentricity effects and focus on the net effects due to ν_e regeneration in the Earth (see the Appendix for further details). We conventionally divide the year in two six-months periods (indicated as “Winter” and “Summer”) centered at the solstice days and separated by the equinox days:

$$\begin{aligned} \text{Winter} &\equiv \text{winter solstice (21 dec.)} \pm 3 \text{ months} \\ &\simeq [23 \text{ september, } 21 \text{ march}] , \end{aligned} \tag{1}$$

$$\begin{aligned} \text{Summer} &\equiv \text{summer solstice (21 jun.)} \pm 3 \text{ months} \\ &\simeq [22 \text{ march, } 22 \text{ september}] . \end{aligned} \tag{2}$$

The neutrino oscillation probabilities and event rates are then averaged over such periods through a “weight function” approach similar to that of Ref. [20], as discussed in the Appendix.

Figure 3 shows the results of our calculation of the gallium absorption rates (in SNU) averaged over winter (R_W), summer (R_S), and year (R_Y), together with the main new result of this work, the winter-summer difference $R_W - R_S$. Since eccentricity effects are removed, the difference $R_W - R_S$ approaches zero in the limits of no oscillations ($\delta m^2 \rightarrow 0$ or $\theta \rightarrow 0$) and of energy-averaged oscillations (large δm^2), up to small round-off errors (see below). The comparison of the two upper panels (R_W and R_S) shows that, in the region of the LOW solution ($\delta m^2 \sim 10^{-7}$), large Earth regeneration effects distort the iso-SNU Gallium curves both in winter and in summer; indeed, the corresponding distortion in the R_Y panel is partly responsible for the appearance of the LOW solution in fits to the data. Notice that, in the region of the LOW solution, the yearly-averaged theoretical rate is $R_Y \sim 60$ SNU, which is consistent with the SAGE results ($\sim 67 \pm 8$ SNU [3]), but somewhat underestimates the GALLEX rate ($\sim 77.5 \pm 8$ SNU [2]). Therefore, the first check of the LOW solution in GNO will come from a more precise measurement of the total rate averaged over the year.

In the fourth panel of Fig. 3, the difference $R_W - R_S$ shows a rather complicated structure as a function of the mass-mixing parameters, with several peaks and valleys. The values of $R_W - R_S$ are almost everywhere positive, since Earth matter effects are typically less pronounced in summer than in winter, when the neutrino trajectories probe the inner part

of the Earth and can cross its core,⁴ as shown in the Appendix. The maximum value of $R_W - R_S$ is 8.3 SNU. However, small negative values (-0.7 SNU at minimum) can be reached around $(\delta m^2/\text{eV}^2, \sin^2 2\theta/\cos 2\theta) \simeq (10^{-7}, 0.7)$, inside the “boomerang-shaped” region labeled by zero. Smaller negative values (tenths of a SNU) can also be reached around $(\delta m^2/\text{eV}^2, \sin^2 2\theta/\cos 2\theta) \simeq (1.5 \times 10^{-7}, 0.003)$.⁵ The outermost curve, labeled ~ 0 SNU, crosses a region at very low gradient, and is thus numerically unstable: very small changes (percents of a SNU) can shift it significantly. All the other isolines are stable, being located in high-gradient regions. Since we estimate a numerical accuracy of about $\lesssim 0.03$ SNU in our total rates, the ~ 0 SNU curve simply indicates a zone with negligibly small winter-summer difference. This zone covers the SMA and LMA regions of Fig. 1. Negative or zero values for the winter-summer difference are instead irrelevant for the LOW solution region, where the difference $R_W - R_S$ is positive and greater than about 4 SNU, with a local maximum of 6.3 SNU. Therefore, if the LOW solution is the explanation of the solar neutrino problem, one should observe in GNO a net winter-summer difference (in excess of the trivial eccentricity difference) of about 4 to 6 SNU. No significant difference should be observed in the case of the SMA or LMA solutions.

In order to understand better the structure of the $R_W - R_S$ isolines, we show in Fig. 4 the separate contributions to this difference coming from the pp , Be, $pep+\text{CNO}$, and B solar neutrino fluxes.⁶ The leading contribution to the winter-summer difference in the LOW region appears to be given by pp neutrinos, with a subleading contribution from Be neutrinos, and negligible contributions from other sources. The δm^2 value at the maximum of each plot roughly scales as $\delta m^2/\langle E_\nu \rangle$, where $\langle E_\nu \rangle$ is the average neutrino energy; therefore, the sum of the various contributions produces separates peaks in the total value of $R_W - R_S$, as already noted in Fig. 3.

Figure 4 demonstrates that the winter-summer asymmetry in GNO is mainly sensitive to pp neutrinos, thus providing a test of the LOW solution intrinsically different from the BOREXINO night-day asymmetry, which is dominated by Be neutrinos. The two tests are also complementary in tracking the origin of the time variations: a possible seasonal signal in GNO, if originated by vacuum (instead of MSW) oscillations, should not produce a $N - D$ asymmetry in BOREXINO.

It is curious to notice that the latitude dependence of the seasonal variations is different from the case of day-night variations, which could be enhanced in an equatorial experiment [12,20,40]. In fact, the difference $R_W - R_S$ vanishes at the equator, while it becomes equal to the night-day rate difference at the poles, where nighttime coincides with winter.

⁴Recent analytical studies of neutrino oscillations along the Earth mantle-core density profile are presented in [38].

⁵Similarly, night-day rate differences can take slightly negative values in some regions of the parameter space [12,39].

⁶In Fig. 4, the isolines labeled “ ~ 0 ” cross (as in Fig. 3) regions at very low gradient, where the values of $R_W - R_S$ is either zero or of the order of the numerical accuracy ($\lesssim 0.03$ SNU).

A final remark about uncertainties is in order. The “theoretical” error in $R_W - R_S$ at GNO, due to systematic uncertainties of the SSM, is very small. In fact, for a typical expected signal $R_W - R_S \simeq 4 \text{ SNU } (pp) + 1 \text{ SNU } (\text{Be})$, the 1σ SSM errors [8] amount to $\sim 0.04 \text{ SNU}$ and $\sim 0.09 \text{ SNU}$ for the pp and Be flux components, respectively. Moreover, since the pp and Be flux errors are strongly anticorrelated [41], the two error components tend to cancel, giving a total theoretical uncertainty as small as $\sim 0.05 \text{ SNU}$. Concerning the experimental errors, they can only be guessed at present. The statistical uncertainty of $R_W - R_S$, given the prospective estimates of [23], should be $\lesssim 2 \text{ SNU}$ after about one solar cycle. The systematics might be dangerously larger [23]; however, their constant components are expected to cancel, to a large extent, in a rate difference such as $R_W - R_S$. A dedicated Monte Carlo simulation would be very helpful to estimate the total errors, and thus the statistical significance, of the $R_W - R_S$ measurement at GNO.

IV. SUMMARY AND PROSPECTS

We have shown that the so-called “LOW” MSW solution to the solar neutrino problem can be tested through Earth regeneration effects in two complementary ways: day-night variations in BOREXINO and seasonal variations in GNO. The first are dominated by Be neutrinos, and the second by pp neutrinos. The net winter-summer difference of event rates in GNO (removing eccentricity effects) amounts to about 4–6 SNU within the LOW solution, and it might be detected in GNO after ~ 10 years of data taking, assuming the progressive error reduction estimated in [23].

In this work we have focussed on six-months averaged GNO rates, in order to compute the seasonal effect corresponding to the largest statistics. Of course, the effect could be larger in selected (shorter) intervals of time, but the corresponding statistics would also be lower. It might be useful to investigate optimal periods for time averaging (maximizing the signal-to-error ratio), when the prospective GNO statistical and systematic uncertainties will be quantified more precisely.

ACKNOWLEDGMENTS

One of us (D.M.) thanks Z. Berezhiani and the organizers of the Gran Sasso Summer Institute “Massive Neutrino in Physics and Astrophysics,” where part of this work was done, for kind hospitality.

APPENDIX A: SOLAR EXPOSURE DURING WINTER AND SUMMER

In this Section we discuss our calculation of the average survival probability $P_{\text{SE}}(E_\nu)$ for a ν_e crossing the Sun (S) and the Earth (E), during winter and summer time. The method is similar to the one used for yearly averaging in Ref. [20], to which we refer the reader for notation, conventions, and details not repeated here.

We define the daily time τ_d as $2\pi \times \text{day}/365$, so that $\tau_d \in [0, 2\pi]$, with $\tau_d = 0$ at winter solstice (21 december). “Winter” (W) is then defined as a period of ± 3 months ($\pm\pi/2$) centered at $\tau_d = 0$, and “Summer” (S) as the complementary period of the year (see also Sec. III). Since the physics is symmetric in the winter half-intervals $[-\pi/2, 0]$ and $[0, \pi/2]$, the time integration interval can be reduced to $[0, \pi/2]$ for winter.

An important quantity, which depends on the latitude λ , is represented by the fraction α of nighttime over the whole day during winter:

$$\alpha = \frac{2}{\pi^2} \int_0^{\pi/2} d\tau_d \arccos[\tan \lambda \tan \delta_S(\tau_d)] , \quad (\text{A1})$$

where δ_S is the sun declination,

$$\sin \delta_S = -\sin i \cos \tau_d , \quad (\text{A2})$$

i being the Earth inclination (0.4901 rad). At the Gran Sasso site ($\lambda = 42.45^\circ$) one gets $\alpha = 0.5795$. The fraction of nighttime during summer is, of course, $1 - \alpha = 0.4205$.

In order to calculate the average Sun-Earth survival probability $\langle P_{\text{SE}} \rangle_W$ over the winter period, it is useful to split such period into nighttime (N) and daytime (D). During daytime, the Earth correction is absent, and only the survival probability in the Sun (P_S) is relevant:

$$\begin{aligned} \langle P_{\text{SE}} \rangle_W &= \alpha \langle P_{\text{SE}} \rangle_{W,N} + (1 - \alpha) \langle P_{\text{SE}} \rangle_{W,D} \\ &= \alpha \langle P_{\text{SE}} \rangle_{W,N} + (1 - \alpha) P_S . \end{aligned} \quad (\text{A3})$$

Similarly, for summer averages one has:

$$\langle P_{\text{SE}} \rangle_S = (1 - \alpha) \langle P_{\text{SE}} \rangle_{S,N} + \alpha P_S , \quad (\text{A4})$$

so that the task is reduced to the calculation of the winter and summer averages during nighttime, $\langle P_{\text{SE}} \rangle_{W,N}$ and $\langle P_{\text{SE}} \rangle_{S,N}$.

Following the approach of Ref. [20], we transform the integrations over winter and summer nighttime in integrations over the nadir angle $\eta \in [0, \pi/2]$ through appropriate weight functions $W_W(\eta)$ and $W_S(\eta)$:

$$\langle P_{\text{SE}} \rangle_{W,N} = \frac{\int_0^{\pi/2} d\eta W_W(\eta) P_{\text{SE}}(\eta)}{\int_0^{\pi/2} d\eta W_W(\eta)} , \quad (\text{A5})$$

$$\langle P_{\text{SE}} \rangle_{S,N} = \frac{\int_0^{\pi/2} d\eta W_S(\eta) P_{\text{SE}}(\eta)}{\int_0^{\pi/2} d\eta W_S(\eta)} . \quad (\text{A6})$$

The weight functions $W_W(\eta)$ and $W_S(\eta)$ simply represent the solar exposure as a function of the nadir angle, namely, they are proportional to the total fraction of time spent by the Sun as it repeatedly crosses (from a “Ptolemaic” viewpoint) a given nadir angle during winter and summer nighttime, respectively.

In order to show the net seasonal effect due to MSW regeneration in the Earth, we remove eccentricity effects by calculating the weight functions for a “circular” Earth orbit. Of course, this implies that the eccentricity ($1/L^2$) effects shall be appropriately removed also from the experimental rates. Notice that the data must be corrected in any case for time-variation studies, in order to account for blank runs, different durations of runs, and for runs crossing the winter-summer separation days (equinoxes). For a circular earth orbit, it turns out that the weight functions can be generally expressed [20] in terms of complete and incomplete elliptic integrals of the first kind, K and F [42]:⁷

$$K(x) = F(\pi/2, x) \quad (\text{A7})$$

$$F(\phi, x) = \int_0^{\sin \phi} \frac{ds}{\sqrt{(1-s^2)(1-x^2 s^2)}}. \quad (\text{A8})$$

Such integrals can be calculated numerically, e.g., through the routines in [43].

We give only the final results for the winter and summer weight functions $W_W(\eta)$ and $W_S(\eta)$ at the Gran Sasso latitude, the derivation being analogous to the case of the annual weight function $W(\eta)$ in [20]:

$$W_W(\eta) = \frac{2 \sin \eta}{\pi^2} \cdot \begin{cases} 0, & 0 \leq \eta < \lambda - i, \\ z^{-1} K(y/z), & \lambda - i \leq \eta \leq \lambda, \\ z^{-1} F(\chi_1, y/z), & \lambda \leq \eta \leq \lambda + i, \\ y^{-1} F(\chi_2, z/y), & \lambda + i \leq \eta \leq \pi/2, \end{cases} \quad (\text{A9})$$

$$W_S(\eta) = \frac{2 \sin \eta}{\pi^2} \cdot \begin{cases} 0, & 0 \leq \eta < \lambda, \\ z^{-1} F(\xi_1, y/z), & \lambda \leq \eta < \lambda + i, \\ y^{-1} F(\xi_2, z/y), & \lambda + i < \eta \leq \pi/2, \end{cases} \quad (\text{A10})$$

In the above equations, the arguments of the functions are defined as follows:

$$z = \sqrt{\sin i \cos \lambda \sin \eta}, \quad (\text{A11})$$

$$y = \sqrt{\sin \left(\frac{i + \lambda + \eta}{2} \right) \sin \left(\frac{i - \lambda + \eta}{2} \right) \cos \left(\frac{i + \lambda - \eta}{2} \right) \cos \left(\frac{i - \lambda - \eta}{2} \right)}, \quad (\text{A12})$$

⁷ Alternatively, one could absorb the correction due to the eccentricity ϵ in the weight functions, and compare with the raw data. In this approach [12,19] (not adopted in this work), there would be a residual (geometrical) winter-summer asymmetry in the absence of neutrino oscillations, and the weight functions $W(\eta)$ should be corrected by an additional term $\pm \epsilon Y(\eta)$ containing elliptic integrals of the third kind; see Appendix D of [20].

$$p = \sin(\lambda - \eta) / \sin i , \quad (\text{A13})$$

$$q = \sin(\lambda + \eta) / \sin i , \quad (\text{A14})$$

$$\chi_1 = \arcsin \sqrt{\frac{q-p}{(1-p)q}} , \quad (\text{A15})$$

$$\chi_2 = \arcsin \sqrt{\frac{1+q}{2q}} , \quad (\text{A16})$$

$$\xi_1 = \arcsin \sqrt{\frac{2p}{p-1}} , \quad (\text{A17})$$

$$\xi_2 = \arcsin \sqrt{\frac{p-1}{2p}} . \quad (\text{A18})$$

The weight functions $W_W(\eta)$ and $W_S(\eta)$, defined in Eqs. (A9, A10), have the following normalization:

$$\int_0^{\pi/2} d\eta W_W(\eta) = \alpha \quad (\text{A19})$$

$$\int_0^{\pi/2} d\eta W_S(\eta) = 1 - \alpha , \quad (\text{A20})$$

and their sum, $W_Y(\eta) = W_W(\eta) + W_S(\eta)$, represents the weight function appropriate for integration over the year.

Fig. 5 shows the winter, summer, and year weight functions in terms of the nadir angle η . Notice that the Earth core is crossed only during winter time, and that trajectories are generally weighted in different ways during winter and summer. This difference implies that the winter-summer asymmetry does not simply depend on different fractions of nighttime in winter (α) and summer ($1 - \alpha$), as derived in [24] in first approximation, and explains why, in general, the day-night and winter-summer asymmetries are not strictly proportional to each other [25]. Notice that the function $W_Y(\eta)$ in Fig. 5 is identical to the function named $W(\eta)$ in [20] (for the Gran Sasso site).

Finally, the calculated values of $\langle P_{SE} \rangle_{W,S}$ (for each given neutrino energy E_ν) are used to compute the winter and summer event rates $R_{W,S}$ in GNO through the equations:

$$R_W = \int dE_\nu \varphi(E_\nu) \sigma(E_\nu) \langle P_{SE}(E_\nu) \rangle_W , \quad (\text{A21})$$

$$R_S = \int dE_\nu \varphi(E_\nu) \sigma(E_\nu) \langle P_{SE}(E_\nu) \rangle_S , \quad (\text{A22})$$

where $\varphi(E_\nu)$ is the solar neutrino energy spectrum [8] and $\sigma(E_\nu)$ is the neutrino absorption cross section in gallium [44].

REFERENCES

- [1] Homestake Collaboration, B. T. Cleveland, T. J. Daily, R. Davis Jr., J. R. Distel, K. Lande, C. K. Lee, P. S. Wildenhain, and J. Ullman, *Astrophys. J.* **496**, 505 (1998).
- [2] GALLEX Collaboration, W. Hampel *et al.*, *Phys. Lett. B* **447**, 127 (1999).
- [3] SAGE Collaboration, J. N. Abdurashitov *et al.*, *Phys. Rev. C* **60**, 055801 (1999).
- [4] Kamiokande Collaboration, Y. Fukuda *et al.*, *Phys. Rev. Lett.* **77**, 1683 (1996).
- [5] Y. Totsuka, in *PANIC'99*, XVth Particles And Nuclei International Conference (Uppsala, Sweden, 1999), to appear; Report available at <http://www-sk.icrr.u-tokyo.ac.jp/doc/sk/pub>
- [6] Y. Suzuki for the Super-Kamiokande Collaboration, in *Lepton-Photon '99*, Proceedings of the XIX International Symposium on Photon and Lepton Interactions at High Energies (Stanford, California, U.S.A., 1999), to appear; transparencies available at <http://lp99.slac.stanford.edu>
- [7] J. N. Bahcall, *Neutrino Astrophysics* (Cambridge University Press, Cambridge, England, 1989).
- [8] J. N. Bahcall, S. Basu and M. Pinsonneault, *Phys. Lett. B* **433**, 1 (1998); see also J. N. Bahcall's homepage, <http://www.sns.ias.edu/~jnb>
- [9] L. Wolfenstein, *Phys. Rev. D* **17**, 2369 (1978); S. P. Mikheyev and A. Yu. Smirnov, *Yad. Fiz.* **42**, 1441 (1985) [*Sov. J. Nucl. Phys.* **42**, 913 (1985)]; *Nuovo Cim. C* **9** (1986), 17.
- [10] M. C. Gonzalez-Garcia, P. C. de Holanda, C. Peña-Garay, and J. W. F. Valle, *hep-ph/9906469*.
- [11] G. L. Fogli, E. Lisi, D. Montanino, and A. Palazzo, in preparation. For preliminary results see G. L. Fogli in *TAUP '99*, VIth International Workshop on Topics in Astroparticle and Underground Physics (Paris, France, 1999), to appear; transparencies available at <http://taup99.in2p3.fr/TAUP99>
- [12] J. N. Bahcall and P. I. Krastev, *Phys. Rev. C* **56**, 2839 (1997).
- [13] N. Hata and P. Langacker, *Phys. Rev. D* **48**, 2937 (1993).
- [14] G.L. Fogli, E. Lisi, and D. Montanino, *Phys. Rev. D* **54**, 2048 (1996).
- [15] A. J. Baltz and J. Weneser, *Phys. Rev. D* **50**, 5971 (1994); **51**, 3960 (1995).
- [16] E. Calabresu, N. Ferrari, G. Fiorentini, and M. Lissia, *Astropart. Phys.* **4**, 459 (1995).
- [17] N. Hata and P. Langacker, *Phys. Rev. D* **56**, 6107 (1997).
- [18] G.L. Fogli, E. Lisi, and D. Montanino, *Astropart. Phys.* **9**, 119 (1998).
- [19] J. N. Bahcall, P. I. Krastev, and A. Yu. Smirnov, *Phys. Rev. D* **58**, 096016 (1998).
- [20] E. Lisi and D. Montanino, *Phys. Rev. D* **56**, 1792 (1997).
- [21] S. P. Mikheyev and A. Yu. Smirnov, in *Moriond '86*, Proceedings of the 6th Moriond Workshop on Massive Neutrinos in Astrophysics and in Particle Physics (Tignes, France, 1986) edited by O. Fackler and J. Trân Thanh Vân (Frontières, Paris, 1986), p. 355.
- [22] L. Oberauer, in *Neutrino '98*, Proceedings of the XVIII International Conference on Neutrino Physics and Astrophysics (Takayama, Japan, 1998), edited by Y. Suzuki and Y. Totsuka; *Nucl. Phys. B (Proc. Suppl.)* **77** (1999), p. 48.
- [23] T. A. Kirsten, in *Neutrino '98* [22], p. 26.
- [24] A. Yu. Smirnov, in *Moriond '99*, Proceedings of the XXXIV Rencontres de Moriond: Electroweak Interactions and Unified Theories (Les Arcs, France, 1999), to appear; *hep-ph/9907296*.

- [25] P. C. de Holanda, C. Peña-Garay, M. C. Gonzalez-Garcia, and J. W. F. Valle, Phys. Rev. D **60**, 093010 (1999).
- [26] J. N. Bahcall, P. I. Krastev, and A. Yu. Smirnov, Phys. Rev. D **60**, 093001 (1999).
- [27] J. N. Bahcall, M. Kamionkowski, and A. Sirlin, Phys. Rev. D **51**, 6146 (1995).
- [28] B. Faïd, G. L. Fogli, E. Lisi, and D. Montanino, Astropart. Phys. **10**, 93 (1999).
- [29] A. M. Dziewonski and D. L. Anderson, Phys. Earth Planet. Inter. **25**, 297 (1981).
- [30] A. de Gouvea, A. Friedland, and H. Murayama, hep-ph/9910286.
- [31] J. Bouchez, M. Cribier, W. Hampel, J. Rich, and D. Vignaud, Z. Phys. C **32**, 499 (1986); M. Cribier, W. Hampel, J. Rich, and D. Vignaud, Phys. Lett. B **182**, 89 (1986); A. J. Baltz and J. Weneser, Phys. Rev. D **35**, 528 (1987); **37**, 3364 (1988).
- [32] R. Raghavan, Phys. Rev. Lett. **78**, 3618 (1997).
- [33] J. Bouchez, in the Proceedings of the VIIIth International Workshop on Neutrino Telescopes (Venice, Italy, 1999), edited by M. Baldo Ceolin (Univ. of Padua, Italy, 1999), p. 127.
- [34] R. E. Lanou, in *Neutrino '98* [22], p. 55.
- [35] M. L. Cherry and K. Lande, Phys. Rev. D **36**, 3571 (1987).
- [36] A. Dar, A. Mann, Y. Melina, and D. Zajfman, Phys. Rev. D **35**, 3607 (1987).
- [37] S. Hiroi, H. Sakuma, T. Yanagida, and M. Yoshimura, Prog. Theor. Phys. **78**, 1428 (1987).
- [38] S. T. Petcov, Phys. Lett. B **434**, 321 (1998); E. K. Akhmedov, Nucl. Phys. B **538**, 25 (1999).
- [39] Q. Y. Liu, M. Maris, and S. T. Petcov, Phys. Rev. D **56**, 5991 (1997); M. Maris and S. T. Petcov, Phys. Rev. D **56**, 7444 (1997).
- [40] J. M. Gelb, W. Kwong, and S. P. Rosen, Phys. Rev. Lett. **78**, 2296 (1997).
- [41] G. L. Fogli and E. Lisi, Astropart. Phys. **3**, 185 (1995).
- [42] I. S. Gradshteyn and I. M. Ryzhik, *Tables of Integrals, Series, and Products* (Academic, San Diego, CA, 1994).
- [43] CERN Program Library CERNLIB, Fortran subroutine package C346 for the calculation of (in)complete elliptic integrals. Documentation available at <http://wwwinfo.cern.ch/asd/cernlib.html>
- [44] J. N. Bahcall, Phys. Rev. C **56**, 3391 (1997).

FIGURES

FIG. 1. Results of our global χ^2 fit [11] for two-neutrino MSW oscillations, including total neutrino event rates from the Chlorine [1], Gallium [2,3], and Water-Cherenkov experiments [4,5], as well as the Super-Kamiokande night-day asymmetry and electron recoil energy spectrum [6]. Neutrino fluxes, spectra and cross sections are taken from [8]. The contours at 90%, 95%, and 99% C.L. correspond to $\Delta\chi^2 = 4.61$, 5.99, and 9.21.

FIG. 2. Expected neutrino event rates in BOREXINO (averaged over one year) during daytime (D), nighttime (N), and full day ($N + D$), together with the night-day asymmetry $N - D/N + D$. Rates are normalized to unoscillated expectations.

FIG. 3. Expected neutrino event rates R in GNO, averaged over “Winter” [23 sep.–21 mar.], “Summer” [22 mar.–22 sep.], and Year, together with the winter-summer difference $R_W - R_S$. All rates are given in SNU. Eccentricity effects are removed, so that $R_W - R_S$ represents the net MSW seasonal effect due ν_e regeneration in the Earth.

FIG. 4. Separate contributions to the winter-summer difference $R_W - R_S$ in GNO due to pp , pep +CNO, and B solar neutrinos. Isolines correspond to integer values of $(R_W - R_S)/\text{SNU}$ in steps of 1 SNU (dotted lines: even values; solid lines: odd values).

FIG. 5. Solar exposure functions vs nadir angle during winter, summer, and the whole year (at the Gran Sasso site). The functions W_Y and W_W coincide for $\eta < \lambda$.

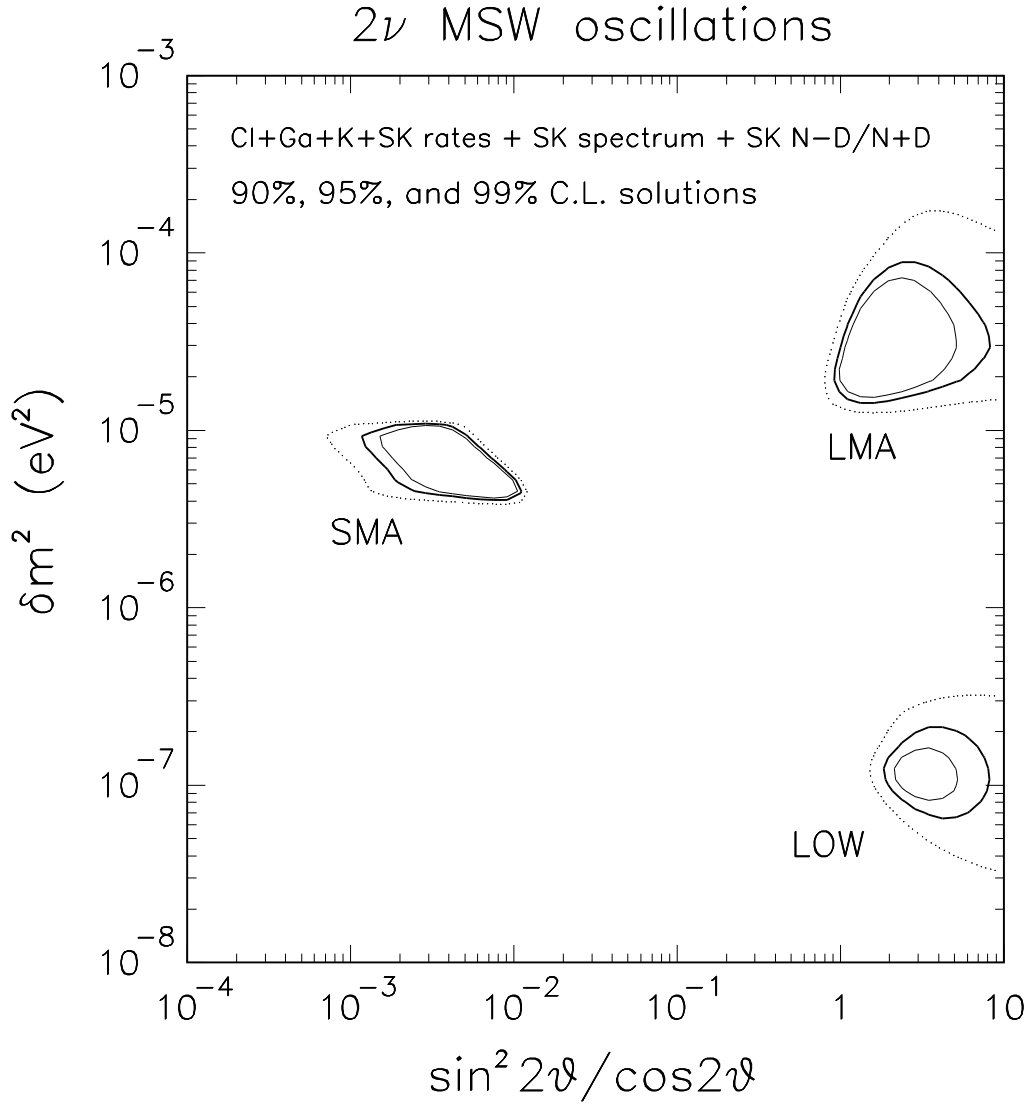


FIG. 1. Results of our global χ^2 fit [11] for two-neutrino MSW oscillations, including total neutrino event rates from the Chlorine [1], Gallium [2,3], and Water-Cherenkov experiments [4,5], as well as the Super-Kamiokande night-day asymmetry and electron recoil energy spectrum [6]. Neutrino fluxes, spectra and cross sections are taken from [8]. The contours at 90%, 95%, and 99% C.L. correspond to $\Delta\chi^2 = 4.61$, 5.99, and 9.21.

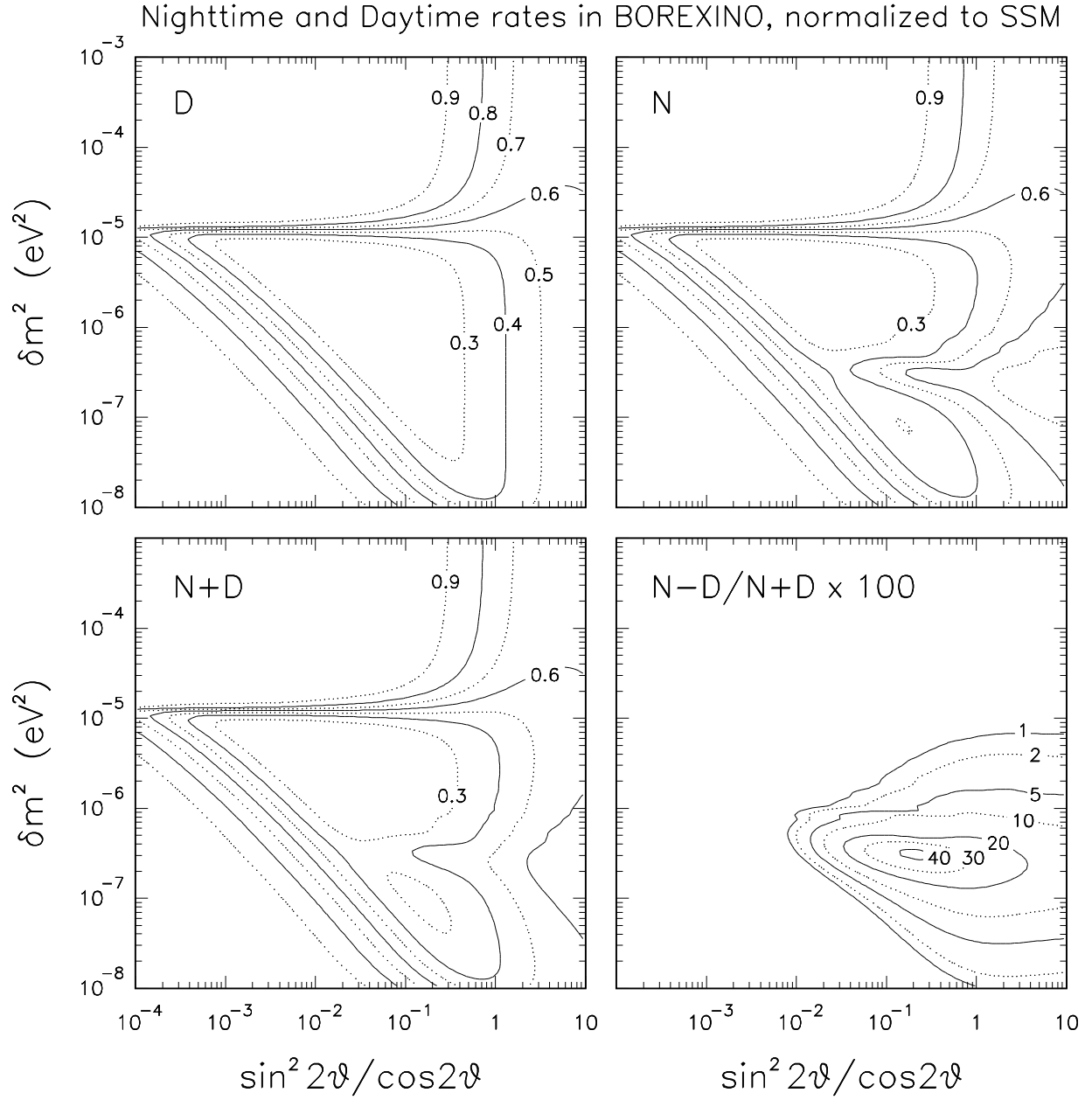


FIG. 2. Expected neutrino event rates in BOREXINO (averaged over one year) during daytime (D), nighttime (N), and full day ($N + D$), together with the night-day asymmetry $N - D/N + D$. Rates are normalized to unoscillated expectations.

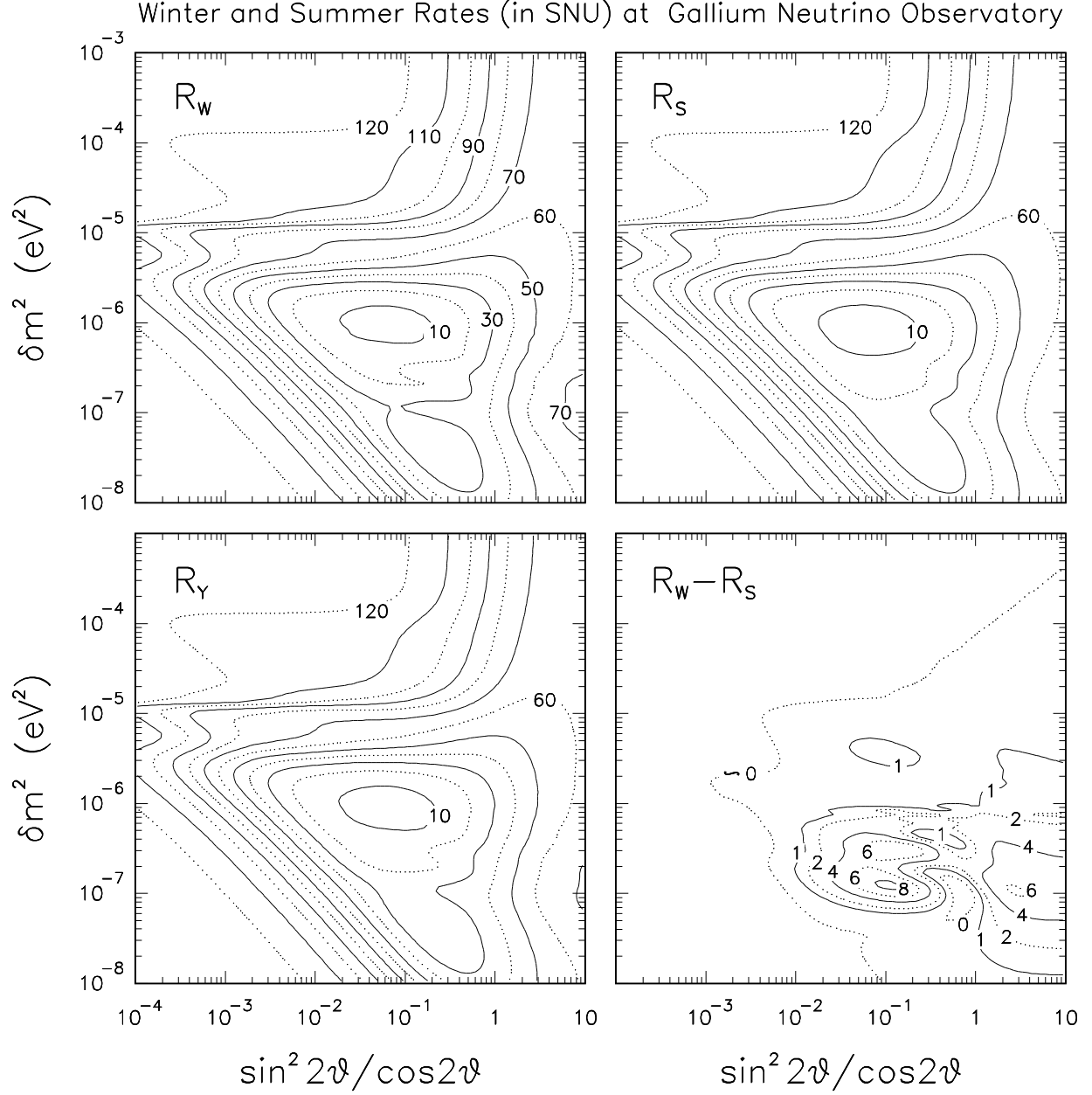


FIG. 3. Expected neutrino event rates R in GNO, averaged over “Winter” [23 sep.–21 mar.], “Summer” [22 mar.–22 sep.], and Year, together with the winter-summer difference $R_W - R_S$. All rates are given in SNU. Eccentricity effects are removed, so that $R_W - R_S$ represents the net MSW seasonal effect due to ν_e regeneration in the Earth.

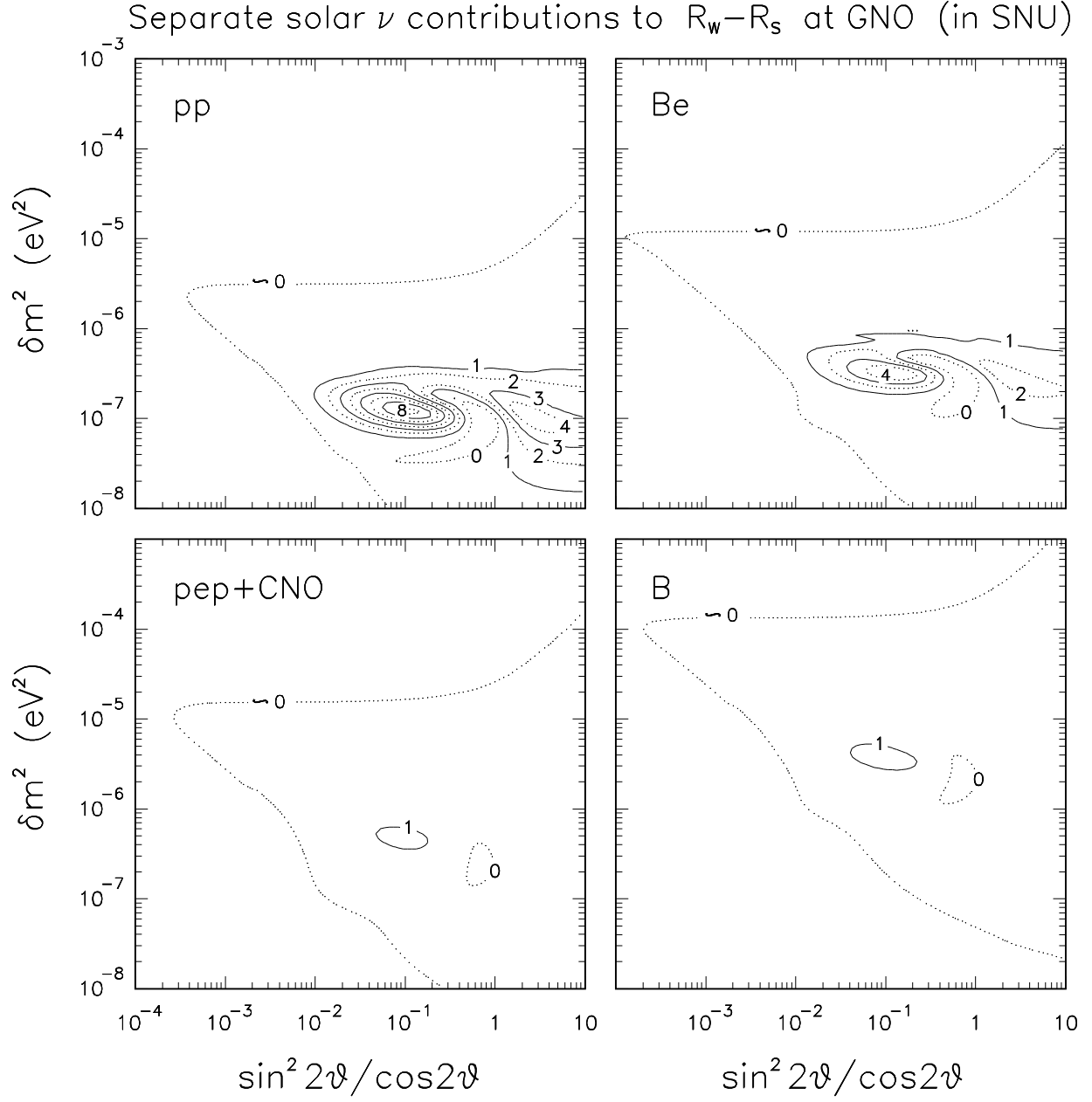


FIG. 4. Separate contributions to the winter-summer difference $R_W - R_S$ in GNO due to pp , $pep+CNO$, and B solar neutrinos. Isolines correspond to integer values of $(R_W - R_S)/\text{SNU}$ in steps of 1 SNU (dotted lines: even values; solid lines: odd values).

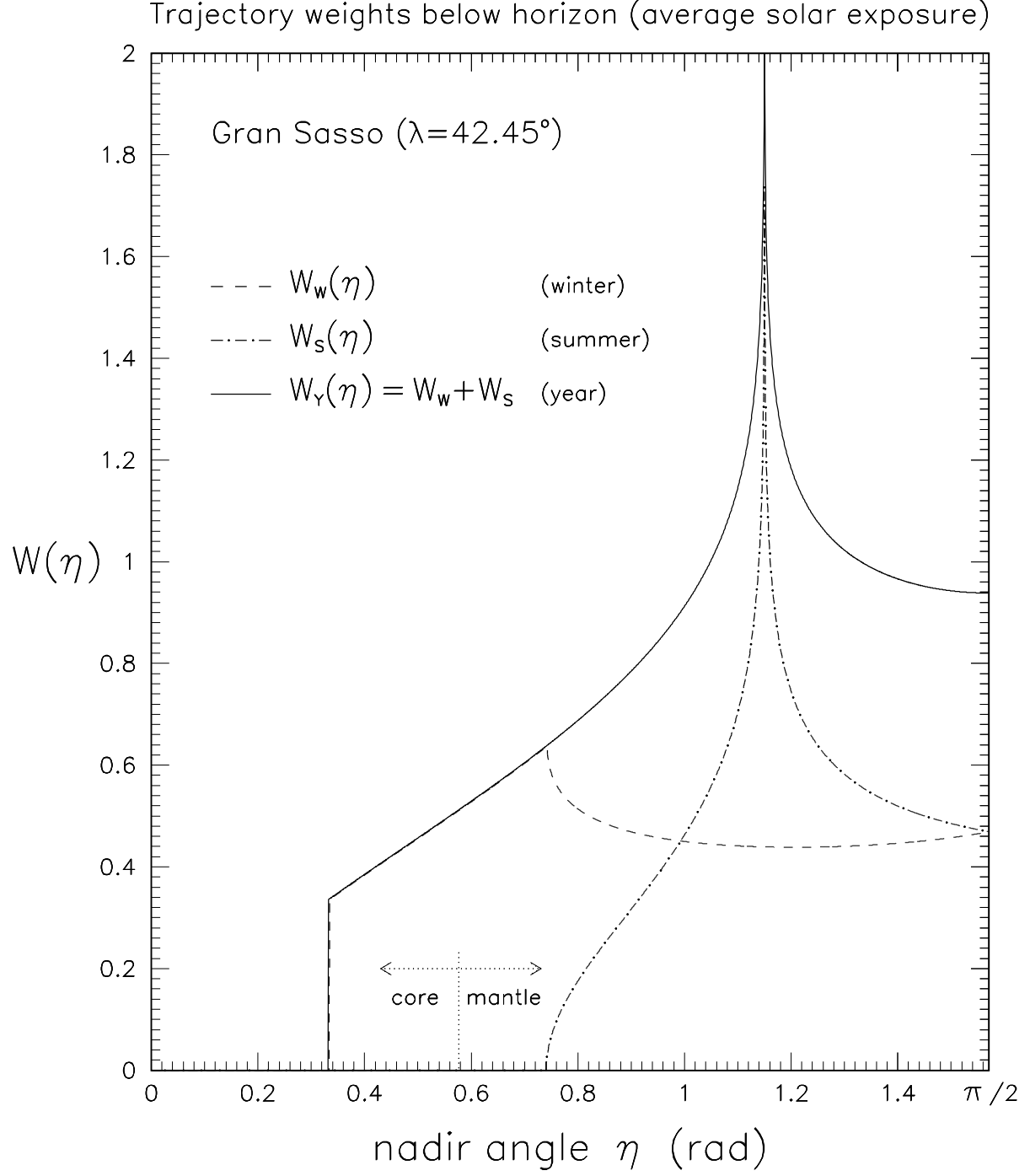


FIG. 5. Solar exposure functions *vs* nadir angle during winter, summer, and the whole year (at the Gran Sasso site). The functions W_Y and W_W coincide for $\eta < \lambda$.